A New MRTD Scheme Based on Coifman Scaling Functions for the Solution of Scattering Problems

Xingchang Wei, Erping Li, *Senior Member, IEEE,* and Changhong Liang, *Senior Member, IEEE*

***Abstract*—This letter describes a new multiresolution time-domain scheme which is developed based on Coifman compactly supported scaling functions with some number of vanishing moments. The highly linear dispersion properties of this scheme are investigated and the two-dimensional and three-dimensional scattering problems are analyzed in order to demonstrate the advantages of this scheme over conventional finite difference time-domain scheme with respect to memory requirements and computing time.**

***Index Terms*—Coifman scaling functions, finite-difference time-domain method (FDTD), multiresolution time-domain analysis (MRTD).**

I. Introduction

THE FINITE difference time-domain (FDTD) method is a powerful numerical technique in electromagnetic field computation [1]; however, it suffers from some limitations, such as the numerical dispersion. To restrain this dispersion for electrically large objects, fineness cells are required, which takes more computer resources and longer computing time. Some development had been made to overcome this limitation such as high-order FDTD schemes [2]. In recent years, the development of wavelet provides a new method to solve such problems [3]. The multiresolution time-domain schemes based on Battle–Lemarie wavelet functions [4], Daubechies wavelet functions [5], and their scaling functions, have been studied and show highly linear dispersion characteristics than convention Yee's scheme did. In this paper, a new multiresolution time-domain analysis (MRTD) scheme based on Coifman scaling functions is derived. In comparison with all of the wavelet and scaling functions used in MRTD schemes available, the Coifman scaling function has its unique Dirac-δ-like sampling property. Therefore, in this MRTD scheme, it is more easy to deal with the connection condition and reconstruct the electromagnetic field using the obtained coefficients.

II. New MRTD Scheme

The Coifman scaling function has been successfully employed in moment methods (MM) to solve electromagnetic field integral equations. The set of Coifman scaling functions $\{\phi(x-i)|i \in \text{integer}\}$ are complete and orthonormal functions. $\phi(x)$ with the order $2N$ has the following unique vanishing moment character:

$$\int_{-\infty}^{\infty} x^p \phi \cdot dx = 0, \qquad p = 1, 2, \ldots, 2N-1$$

and

$$\int_{-\infty}^{\infty} \phi \cdot dx = 1. \tag{1}$$

So, $\phi(x)$ exhibits the Dirac-δ-like sampling property for a smooth function $f(x)$ under L^2 norm, that is $\int_{-\infty}^{\infty} f(x)\phi(x)\,dx \approx f(0)$.

Using the set of Coifman scaling functions in space and pulse functions in time, as the expansion and test functions [6], the Galerkin method is applied to discretify Maxwell's equations in perfectly matched layer (PML) [1]. The following MRTD scheme based on Coifman scaling functions can be obtained:

$$E_{xy}|^n_{i+(1/2),\,j,\,k} = c_1(y)\cdot E_{xy}|^{n-1}_{i+(1/2),\,j,\,k} + c_2(y) \cdot \sum_{l=2-6N}^{6N-1} a(l)\cdot H_z|^{n-(1/2)}_{i+(1/2),\,j+(1/2)-l,\,k} \tag{2.1}$$

$$E_{xz}|^n_{i+(1/2),\,j,\,k} = c_1(z)\cdot E_{xz}|^{n-1}_{i+(1/2),\,j,\,k} - c_2(z) \cdot \sum_{l=2-6N}^{6N-1} a(l)\cdot H_y|^{n-(1/2)}_{i+(1/2),\,j,\,k+(1/2)-l} \tag{2.2}$$

$$E_{yz}|^n_{i,\,j+(1/2),\,k} = c_1(z)\cdot E_{yz}|^{n-1}_{i,\,j+(1/2),\,k} + c_2(z) \cdot \sum_{l=2-6N}^{6N-1} a(l)\cdot H_x|^{n-(1/2)}_{i,\,j+(1/2),\,k+(1/2)-l} \tag{2.3}$$

$$E_{yx}|^n_{i,\,j+(1/2),\,k} = c_1(x)\cdot E_{yx}|^{n-1}_{i,\,j+(1/2),\,k} - c_2(x) \cdot \sum_{l=2-6N}^{6N-1} a(l)\cdot H_z|^{n-(1/2)}_{i+(1/2)-l,\,j+(1/2),\,k} \tag{2.4}$$

$$E_{zx}|^n_{i,\,j,\,k+(1/2)} = c_1(x)\cdot E_{zx}|^{n-1}_{i,\,j,\,k+(1/2)} + c_2(x) \cdot \sum_{l=2-6N}^{6N-1} a(l)\cdot H_y|^{n-(1/2)}_{i+(1/2)-l,\,j,\,k+(1/2)} \tag{2.5}$$

Manuscript received November 16, 2001; revised May 6, 2002.

X. Wei and E. Li are with the Computational Electromagnetics and Electronics Division, Institute of High Performance Computing, Science Park II, Singapore.

C. Liang is with the Department of Electrical Engineering, Xidian University, Xi'an, Shaanxi, China.

Digital Object Identifier 10.1109/LMWC.2002.804562.

$$E_{zy}|^{n}_{i,\,j,\,k+(1/2)} = c_1(y)\cdot E_{zy}|^{n-1}_{i,\,j,\,k+(1/2)} - c_2(y) \cdot \sum_{l=2-6N}^{6N-1} a(l)\cdot H_x|^{n-(1/2)}_{i,\,j+(1/2)-l,\,k+(1/2)} \tag{2.6}$$

$$H_{xy}|^{n+(1/2)}_{i,\,j+(1/2),\,k+(1/2)} = c_3(y)\cdot H_{xy}|^{n-(1/2)}_{i,\,j+(1/2),\,k+(1/2)} - c_4(y) \cdot \sum_{l=2-6N}^{6N-1} a(l)\cdot E_z|^{n}_{i,\,j+1-l,\,k+(1/2)} \tag{2.7}$$

$$H_{xz}|^{n+(1/2)}_{i,\,j+(1/2),\,k+(1/2)} = c_3(z)\cdot H_{xz}|^{n-(1/2)}_{i,\,j+(1/2),\,k+(1/2)} + c_4(z) \cdot \sum_{l=2-6N}^{6N-1} a(l)\cdot E_y|^{n}_{i,\,j+(1/2),\,k+1-l} \tag{2.8}$$

$$H_{yz}|^{n+(1/2)}_{i+(1/2),\,j,\,k+(1/2)} = c_3(z)\cdot H_{yz}|^{n-(1/2)}_{i+(1/2),\,j,\,k+(1/2)} - c_4(z) \cdot \sum_{l=2-6N}^{6N-1} a(l)\cdot E_x|^{n}_{i+(1/2),\,j,\,k+1-l} \tag{2.9}$$

$$H_{yx}|^{n+(1/2)}_{i+(1/2),\,j,\,k+(1/2)} = c_3(x)\cdot H_{yx}|^{n-(1/2)}_{i+(1/2),\,j,\,k+(1/2)} + c_4(x) \cdot \sum_{l=2-6N}^{6N-1} a(l)\cdot E_z|^{n}_{i+1-l,\,j,\,k+(1/2)} \tag{2.10}$$

$$H_{zx}|^{n+(1/2)}_{i+(1/2),\,j+(1/2),\,k} = c_3(x)\cdot H_{zx}|^{n-(1/2)}_{i+(1/2),\,j+(1/2),\,k} - c_4(x) \cdot \sum_{l=2-6N}^{6N-1} a(l)\cdot E_y|^{n}_{i+1-l,\,j+(1/2),\,k} \tag{2.11}$$

$$H_{zy}|^{n+(1/2)}_{i+(1/2),\,j+(1/2),\,k} = c_3(y)\cdot H_{zy}|^{n-(1/2)}_{i+(1/2),\,j+(1/2),\,k} + c_4(y) \cdot \sum_{l=2-6N}^{6N-1} a(l)\cdot E_x|^{n}_{i+(1/2),\,j+1-l,\,k} \tag{2.12}$$

where

$$c_1(i) = \frac{2\varepsilon - \Delta t\cdot\sigma_i}{2\varepsilon + \Delta t\cdot\sigma_i}, \qquad c_2(i) = \frac{2\Delta t}{\Delta(2\varepsilon + \Delta t\cdot\sigma_i)},$$
$$c_3(i) = \frac{2\mu - \Delta t\cdot\sigma_i^*}{2\mu + \Delta t\cdot\sigma_i^*}, \qquad c_4(i) = \frac{2\Delta t}{\Delta(2\mu + \Delta t\cdot\sigma_i^*)}$$

$i = x, y, z$, and ε, μ, σ_i, and σ_i^* are the permittivity, permeability, electric conductivity, and magnetic loss of the medium respectively. Δt and Δ represent the time and space discretization intervals, respectively. $E_x|^{n}_{i+1/2,\,j,\,k}$, $E_y|^{n}_{i,\,j+1/2,\,k}$, $E_z|^{n}_{i,\,j,\,k+1/2}$, $H_x|^{n-(1/2)}_{i,\,j+1/2,\,k+1/2}$, $H_y|^{n-(1/2)}_{i+1/2,\,j,\,k+1/2}$, and $H_z|^{n-(1/2)}_{i+1/2,\,j+1/2,\,k}$ are the unknown coefficients in electromagnetic field expansion equations. They can be split into two subcomponents as in equations (2.1)–(2.12). $2N$ is the order of $\phi(x)$. $a(l)$ can be obtained by numerical integrals. Since $\phi(x)$ is compactly supported and has some numbers of vanishing moments, the number of $a(l)$ is finite and $a(l)$ decays quickly when $|l|$ becomes larger. Table I illustrates $a(l)$ related to $\phi(x)$ with 4-order and 8-order, where, $a(l)$ with $l \le 0$ can be obtained by the symmetry relation $a(l) = -a(1-l)$, which are not listed in the Table. In the following examples, the Coifman scaling function with 4-order is used.

TABLE I
COEFFICIENTS $a(l)$

l	Coif4	Coif8
1	-1.31176	-1.30666
2	0.15757	0.16494
3	-0.04383	-0.06042
4	0.00982	0.02429
5	-0.00124	-0.00857
6	0.00005	0.00243
7	NA	-0.00053
8	NA	0.00009

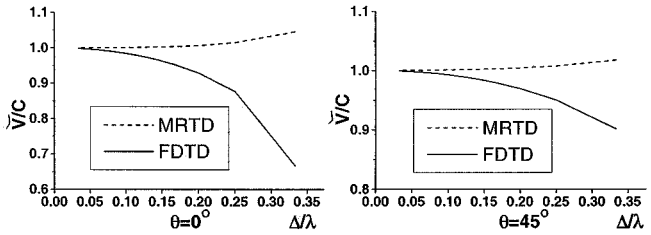

(a) (b)

Fig. 1. Variation of the numerical phase velocity $\bar{v}$ with grid size.

As $\phi(x)$ has the Dirac-δ-like sampling property, all those unknown coefficients in (2.1)–(2.12) can be taken as the samples of the relative continuous field components in space, as well as in time. By giving the initial value of the field, these coefficients can be obtained iteratively. On the other hand, when we need to find out the incident field such as $E_{x,\,inc}|^{n}_{i+(1/2),\,j,\,k}$ near the connection interface, which divides the computation region into total-field region and scattered-field region, no numerical integral, including continuous $E_{x,\,inc}(x,\,y,\,z,\,t)$, is needed, because we can take the samples of $E_{x,\,inc}(x,\,y,\,z,\,t)$ at point $[(i+1/2)\Delta,\,j\Delta,\,k\Delta,\,n\Delta t]$ as $E_{x,\,inc}|^{n}_{i+1/2,\,j,\,k}$. This makes the (2.1)–(2.12) more easy to use. Note that if electromagnetic field components are expanded by pulse functions, both in space and time, using the Galerkin method, the Yee's FDTD scheme can be achieved with $a(0) = 1$, $a(1) = -1$, and $a(l) = 0$ for other l.

Fig. 1(a) and (b) shows the variation of the numerical phase velocity $\tilde{v}$ with grid size for conventional FDTD scheme and this MRTD scheme when $\theta = 0°$ and $\theta = 45°$, respectively. Here, the incident wave is a TE plane wave travelling in free-space with the field components E_x, E_y, and H_z, θ is the propagation angle with respect to the positive x-axis, $c\cdot\Delta t/\Delta = 1/4$, and c is the free-pace speed of light. It can be observed from the figures that

1) the phase velocity error is getting larger when $\theta = 0°$ than when $\theta = 45°$, for both FDTD and MRTD schemes;
2) the numerical phase velocity in MRTD is greater than c, while it is less than c in FDTD;

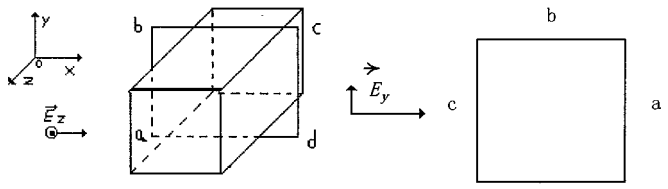

Fig. 2. Scatters and incident wave.

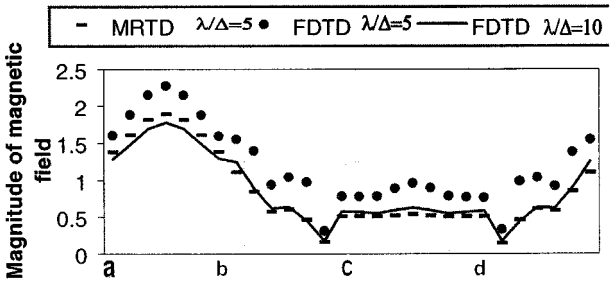

Fig. 3. Magnitude of the magnetic field.

3) in all, the phase velocity error in MRTD is less than that in FDTD. So, the grid resolutions in MRTD can be more coarse.

III. Numerical Examples

The performance of the MRTD is examined using a conducting cube and square cylinders, where the scatters and the incident wave are shown in Fig. 2(a) and (b). In following examples, $c\Delta t/\Delta$ is 1/4 and the dimension of scatters are uniformed by the wavelength of the incident wave λ. The incident waves are sinusoidal plane waves.

Fig. 3(a) illustrates the magnitude of the magnetic field which is parallel to the line $abcd$, as shown in Fig. 2(a). The line $abcd$ is in the center of the cube with respect to z-axis and $\lambda/10$ away from the four surfaces of the cube, which is of $1.2\lambda \times 1.2\lambda \times 1.2\lambda$. Fig. 3(b) shows the magnitude of magnetic field, which is $\lambda/10$ away from the cylinder, where the square cylinder is of $8\lambda \times 8\lambda$. We can see that the magnetic field error is larger for FDTD when the grid size becomes large because of the numerical dispersion. While for MRTD, the solution still agrees well with that obtained by FDTD with fineness grids when the grid size is large.

Table II shows the CPU time, the number of grids, and the error for cylinders using two different methods: MRTD with $\lambda/\Delta = 5$ and FDTD with $\lambda/\Delta = 20$, where the relative error refers to the error between the current obtained by MM, and the current obtained by FDTD or MRTD. The results by MRTD with $\lambda/\Delta = 5$ and FDTD with $\lambda/\Delta = 10$ are compared for the cube in Table III, where the relative error refers to the magnetic field error shown in Fig. 3(a) between FDTD and MRTD. We can see that for the same scatter, MRTD uses less grids than FDTD in achieving the same accuracy and MRTD reduces the computing time, as well.

TABLE II
CPU Time, the Number of Grids and the Error for Cylinders

Perimeter of the cylinder	MRTD			FDTD		
	16λ	24λ	32λ	16λ	24λ	32λ
Number of grids	17 424	20 164	23 104	48 400	67 600	90 000
CPU time(Sec.)	126.38	160.49	196.52	222.06	299.89	406.17
Relative error(%)	8.65	9.37	11.45	5.16	5.91	7.18

TABLE III
CPU Time, the Number of Grids and the Error for the Cube

	Number of grids	CPU time(Min.)	Relative error(%)
MRTD	343 000	1 083	8.3
FDTD	1 560 896	1 963	

IV. Conclusion

A new MRTD scheme based on Coifman scaling functions is derived in this paper. Because of the vanishing moment and the compact support characteristics of the Coifman scaling function, the MRTD scheme is easier to use than other MRTD schemes. Through numerical examinations, it is shown that the new MRTD has highly linear dispersion characteristics and can reduce memory requirements and computing time in comparison to the conventional FDTD method. It should be noted that, as discussed in many papers about MRTD [4], [5], MRTD schemes have somewhat less stability than conventional FDTD. But, this does not discount the MRTD performance as shown in above examples.

References

[1] A. Taflove, *Computational Electrodynamics—The Finite-Difference Time-Domain Method*. Norwood, MA: Artech House, 1995.
[2] T. Deveze, L. Beaulie, and W. Tabbara, "A fourth order scheme for the FDTD algorithm applied to Maxwell equations," in *IEEE A&P Soc. Int. Symp. Dig.*, Chicago, IL, July 1992, pp. 346–349.
[3] W. Xingchang, "Application of wavelet analysis to computational electromagnetics," Ph.D. dissertation, Xidian Univ., Xi'an, P.R. China, Mar. 2001.
[4] M. Krumpholz and L. P. B. Katechi, "MRTD: New time-domain schemes based on multiresolution analysis," *IEEE Trans. Microwave Theory Tech.*, vol. 44, pp. 555–570, Apr. 1996.
[5] Y. W. Cheong, Y. M. Lee, and K. H. Ra *et al.*, "Wavelet-Galerkin scheme of time-dependent inhomogeneous electromagnetic problems," *IEEE Microwave Guided Wave Lett.*, vol. 9, pp. 297–299, Aug. 1999.
[6] X. Wei and C. Liang, "Using the MRTD based on Coifman scaling functions to solve the problem of scattering," *ACTA Electronica Sinica*, 2001, to be published.